Construction and Building Materials 361 (2022) 129602

Contents lists available at ScienceDirect

Construction and Building Materials

journal homepage: www.elsevier.com/locate/conbuildmat

Review

Study of physical and mechanical properties of aerogel-modified expanded perlite aggregate and clay (AEP/C) board

Elif Mercan [*,1], Semiha Yilmazer

Department of Interior Architecture and Environmental Design, Faculty of Art, Design and Architecture, Bilkent University, 06800 Ankara, Turkey
UNAM-National Nanotechnology Research Center, Bilkent University, 06800 Ankara, Turkey

ARTICLE INFO

Keywords:
Clay
Expanded perlite aggregate
Silica aerogel
Sol–gel method

ABSTRACT

The aerogel-modified expanded perlite aggregate and clay (AEP/C) composite boards were produced, and physical and mechanical properties were investigated. The aerogel modification of expanded perlite aggregate was carried out with optimization of the two-step acid-base catalyzed sol–gel method. The perlite shrinkage under high-temperature annealing was prevented by covering perlite surfaces with aerogel modification. The boards with aerogel-modified expanded perlite aggregate (AEP) wrapped by clay matrix were successfully produced. The unit volume mass (UVM) and specific gravity (SG) of AEP/C boards slightly increased to 0.55 ± 0.01 g/cm^3 and 2.36 ± 0.01, respectively. On the other hand, produced AEP/C boards' volume of voids of 36.23 ± 1.05 and water absorption (WA) of 83.91 ± 0.49 % were moderately lower than EPA/C. The mechanical strength of the AEP/C composite boards remained almost unchanged with 0.73 ± 0.04 N/mm^2, and the aerogel modification had practically no effect on the mechanical strength of composite boards.

1. Introduction

An upsurge in global energy consumption results from a striking increase in urban and industrial activities depending on the rapid growth of population size [1]. The energy need in developing countries has increased since new building constructions [2]. The diminished energy needs ensure the availability of energy for others, the ascending rate of demand for power generating plants, restraining the pollution, and the transfer of resources to future generations [3,4]. Depending on the increasing environmental pollution and climate change concerns, the energy efficiency in buildings and construction sustainability have become more apparent [5,6] Effective thermal insulation in buildings has an essential share in lowering the energy demand in the building sector [7]. Especially energy-saving wall insulation materials are prominent in energy conservation in buildings [8–10]. The high thermal insulation performance, desired moisture, and fire resistance, is mainly observed in inorganic insulation materials. On the other hand, organic insulation materials are renewable and environmentally friendly. The mechanical performance of materials is determined according to the material's chemical bonding and form. Therefore, studies focus on enhancing the thermal behavior while eliminating the adverse properties of insulation materials by designing composites [3].

Expanded perlite aggregate is produced by heating the perlite volcanic rock to its softening temperature. The water in perlite grains is vaporized under heating temperatures of 700–1200 °C, and perlite can be extended to a volume of up to 15–20 times its initial size [11]. EPA is a prominent low-cost, chemically inert, soundproof, and fireproof construction material with superior thermal insulation performance and a substantial particle size range [12]. It is used as an aggregate in mortar, plaster, brick, or concrete type of building materials, for example, as loose-fill insulation in building cavities, wallboard, and lightweight fire-resistant coatings [13]. Current applications are fronted on composites to upgrade the materials' physical and mechanical properties via EPA substitution or addition in cementitious materials, using EPA as media for polymers or binders [13,14]. Depending on the cellular structure, it is also suitable for composite production with other materials such as fumed silica and paraffin inside the open pores of EPA [15–17]. The inclusion of EPA in cementitious materials pointed to the reduction of unit weight and density of the mixture, thus using it for the production of lightweight mortar, concrete, plaster, brick, etc. [18–21]. On the other hand, the cellular structure and closed cells of the EPA provide progressive crushing characteristics that cause a decrease in the mechanical strength of the composite [22–24].

* Corresponding author.
E-mail addresses: elif.mercan@bilkent.edu.tr (E. Mercan), semiha@bilkent.edu.tr (S. Yilmazer).
[1] ORCID: 0000-0003-0037-8989.

https://doi.org/10.1016/j.conbuildmat.2022.129602
Received 14 July 2022; Received in revised form 20 September 2022; Accepted 25 October 2022
Available online 10 November 2022

Abbreviations

Nomenclature

b	Board width
d	Board thickness
F	Total force applied to the board (N)
l	Board length (cm)
L	Distance between supports (mm)
m	Board weight (g)
V	Board volume (cm^3)
V_T	Total volume (cm^3)
V_C	Volume change in the flask
V_V	Volume of voids (cm^3)
W	Weight (g)
WA	Water absorption
W_D	Initial weight of dry sample (g)
W_W	Wet weight (g)
ρ	Density (g/cm^3)
σ	Bending strength, flexural strength

Acronyms

AEP	Aerogel-modified expanded perlite
AEP/C	Aerogel-modified expanded perlite/clay
ASR	Alkali-silica reaction
DH_2O	Distilled water
EtOH	Ethanol
EPA	Expanded perlite aggregate
EPA/C	Expanded perlite aggregate/clay
SG	Specific gravity
SiO_2	Silica
TEOS	Tetraethyl orthosilicate
TMCS	Trimethylchlorosilane
UVM	Unit volume mass

The emergence of aerogel, a 3D solid network with distinguished properties, pioneered combining this material with traditional insulation materials. Aerogel is the lightest material with high porosity, low thermal conductivity, excellent fire resistance, and transparent to opaque optical properties [9]. The production chance with many methods and in various forms provides availability of this material and widespread usage of it [25,26]. On the other hand, the fragility of aerogel and high production expenditure cause an adverse effect on the proliferation of its usage in construction [27]. The compressive strength and elastic moduli are sensitive to the environment of aerogels because the crack formation in the structure depends on the synthesis process [28]. Therefore, strengthening of aerogels by avoiding a cracked solid network during production is achieved by controlling parameters through synthesizing routes [29,30]. The contemporary approach in aerogel studies is to solve aerogel's physical and mechanical problems, synthesize the aerogel at a reasonable cost and combine its outstanding properties with other insulation materials like a composite [31]. Additionally, aerogel-filled composites help lower the cost of synthesis and require less time to produce than aerogels [32]. A promising approach in recent studies uses SiO_2 aerogel as reinforced material in the EPA [33]. In many studies, aerogel is synthesized inside the open pores of EPA by adding a source material, silica, during the phases [25,28,34]. Both the disadvantage that arose from high water absorption of EPA is reduced, and the fragility problem of aerogel is overcome with the help of the skeleton of EPA [8]. The surface characteristics, pore, volume, and property correlations were discussed with the microstructure of the composite at an experimental level [27,35]. While researches show that the source material and production method used determine the properties of the aerogel obtained, they also cause curiosity about the effect of using this composite in different matrices on the total physical and mechanical properties.

The direct use of aerogel-modified expanded perlite in buildings does not seem possible due to the inability to reach the target strength limit values or allow mass production. For this reason, research were commonly concentrated on studying the physical and mechanical properties of aerogel-modified expanded perlite embedded into a matrix. The problem of low mechanical strength and high cost of aerogel-based building materials have been solved by Si aerogel/EPA composite reinforcement on different materials. Chen et al. [8] investigated the influence of Si aerogel/EPA composite substitution on the mechanical behaviors of fly ash-based lightweight wall material (LWM). The results revealed that the density of the composite was 335 kg/m^3 and the increment of Si aerogel/EPA composite amount causes a weakening of the compressive strength to 0.88 MPa. Wang et al. [33] examined the performance of concrete prepared by aerogel-filled EPA addition. While the aerogel-filled EPA amount increased, the mechanical strength reduced to 3.71 MPa. Recently, Jia and Li [36] studied the mechanical behavior of cement-based aerogel/EPA composites. The dry densities of composites were 524–951 kg/m^3 and compressive strengths varied from 3.79 to 14.47 MPa according to the preparation of the composites. The study examined the importance of reducing the hydrophobic nature of aerogel to obtain homogenous AEP and the cement matrix slurry for better workability. Despite the studies on aerogel-filled EPA composite substitution on several but mainly cementitious materials, the alkali-silica reaction (ASR) is the origin of deterioration in concrete over time. Clay has no side effects such as ASR and is a low-cost material as matrix/binder in composites [37]. Nevertheless, a few studies of EPA board composite with clay matrix had found in the literature [21,37,38]. Topçu and Işıkdağ [38] stated that the exchange amount of perlite increased, unit weight of the brick decreased. On the other hand, the ascending ratio of perlite led to the shrinking of the brick because of the different shrinkage values of perlite and clay at 900 °C. The maximum shrinkage ratio of 9.5 % of the standard brick allowed to use of 30 % perlite in brick production. This ratio brought 2.0 MPa compressive strength. Yılmazer and Baytekin [37] presented the optimization of the synthesis process and the strength of the self-supporting EPA/clay insulation board. The unit volume mass of the board prepared with 70 % perlite and 30 % clay mixture ratio was 0.215 g/cm^3, and the bending strength was 0.34 N/mm^2. The study said that the thermal resistance of porous materials resulted in low UVM values. Therefore, the UVM of the boards was calculated for EPA/clay, rock wool, and glass fiber reinforced EPA/clay boards. The boards showed lower bending strength values up to 0.16 N/mm^2 due to the reinforcement. Yilmazer [39] determined the optimum ratio as 95 % EPA and 5 % clay by volume, the board had 0.27 g/cm^3 UVM with the bending strength of 0.52 N/mm^2. One of the most critical discussions in the study is that the heating process up to 850–1000 °C caused the sintering of EPA. This led to the shrinkage of the particles during the curing process and disruption of the solid/void ratio, thus deteriorating the bonding of particles and the clay matrix. This can result in cracks in the structure of the insulation boards, and mechanical strength can follow the ascending trend. Studies propose using additional materials such as rock wool fiber to develop the material flexibility and increase the strength of the boards; however, the silane pre-treatment was required to make the fibers hydrophobic [37,39]. Results demonstrated that hydrophobicity causes agglomeration of the fibers and decreased ionic bonding between the composite ingredients.

The aim of the presented work was to produce aerogel-modified expanded perlite/clay (AEP/C) composite board by coping with the synthesis optimizations, and to investigate its physical and mechanical

Table 1
The chemical contents of the EPA and the clay [39,40].

Chemical contents	Composition (%)	
	EPA	Clay
SiO_2	71.0–75.0	56.29
AlO_3	12.5–18.0	14.62
NaO_3	2.9–4.0	
K_2O	0.5–5.0	3.25
CaO	0.5–0.2	13.33
Fe_2O_3	0.1–1.5	7.02
MgO	0.2–0.5	2.86
TiO_2	0.03–0.2	0.74
MnO	0.0–0.1	0.19
SO_3	0.0–0.2	0.11
FeO	0.0–0.1	
Cr	0.0–0.1	
Ba	0.0–0.05	
PbO	0.0–0.3	
Na_2O		1.06

properties. Firstly, the non-hydrophobic aerogel synthesis process was optimized systematically. Subsequently, the amount of perlite for the aerogel-modified expanded perlite (AEP) synthesis was determined. It is known that the shrinkage behavior of expanded perlite in boards causes damages that are difficult to avoid under higher temperature annealing. The sintering of perlite was prevented by aerogel modification. The non-homogeneous slurry mixture problem that was mentioned in previous studies was solved by non-hydrophobic aerogel synthesis inside and on the surface of the expanded perlite. Chemical compatibility between the AEP and clay was examined in the slurry mixing step. The microstructure of the EPA/C and AEP/C were characterized with the scanning electron microscope (SEM). The UVM ratios, specific gravities (SG), the volume of voids, and water absorption (WA) capacity were calculated for EPA/C and AEP/C boards. The bending strength of the boards was tested with a three-point flexural strength principle bending test machine. This work presents a novel method for optimizing the aerogel modification of perlite (AEP) and also producing aerogel-modified expanded perlite and clay (AEP/C) composite board.

2. Experimental

2.1. Materials

Tetraethyl orthosilicate (TEOS, $Si(OC_2H_5)$, Merck, $\geq$ 99.0 % (a/a)) as a Si source, oxalic acid dihydrate as acid catalyst ($C_2H_6O_6$, Merck, 99.5–102.0 %) and ammonia as base catalysts (NH_4OH) were used. Ethanol (EtOH, CH_3CH_2OH, Merck), distilled water (DH_2O), *n*-hexane (C_6H_{14}, Merck), and trimethylchlorosilane (TMCS, $(CH_3)_3$ SiCl, Merck) were other reagents. Expanded perlite aggregate (EPA) with $<$ 3 mm particle size was obtained from Persan Perlite Inc., and ready-made clay is from Güray Seramik Inc. (Avanos, Nevşehir) located in Turkey. The chemical composition of clay and EPA used in this study are shown in Table 1.

2.2. Preparation of SiO_2 aerogel

In this experiment, EPA needs the time to absorb SiO_2 hydrosol before gelation. After the absorption period, the gelation occurs inside and around EPA. Therefore, the low-cost, two-step acid-base catalyzed sol–gel method was used to assure sufficient time for EPA to absorb the hydrosol adequately. In the sol–gel method, determining the concentration and amount of acid and base catalysts is significant to provide enough gelation time and produce qualified aerogel. After the synthesis is completed, the optimization step for AEP preparation is started. The flow chart of the design of the study is illustrated in Fig. 1.

To determine *the concentration of oxalic acid*, all molar ratios were fixed, and the concentration of acid catalyst was altered systematically. The aerogels were prepared by keeping the molar ratio of TEOS:EtOH:H_2O constant at 1:5:7, and the concentration of the ammonia base catalyst was set at 1 M [34]. The acid catalyst was gradually increased by 0.001 from 0.001 M to 0.02 M. The experiments with 0.001 to 0.009 M acid catalyst showed no gelation despite long aging times for days. On the other hand, the gelation started in experiments prepared with 0.01 M; however, gelation required extended aging periods. The gelation took place in a day for the experiments prepared with 0.02 M. Additionally; the pH measurements were carried out while the acid catalyst addition. The pH dependence under acid catalyst additions confirms the condensation reaction and verifies the network formation. The pH results were parallel to the ideal relative reaction rate in the hydrolysis graph in the literature [41,42].

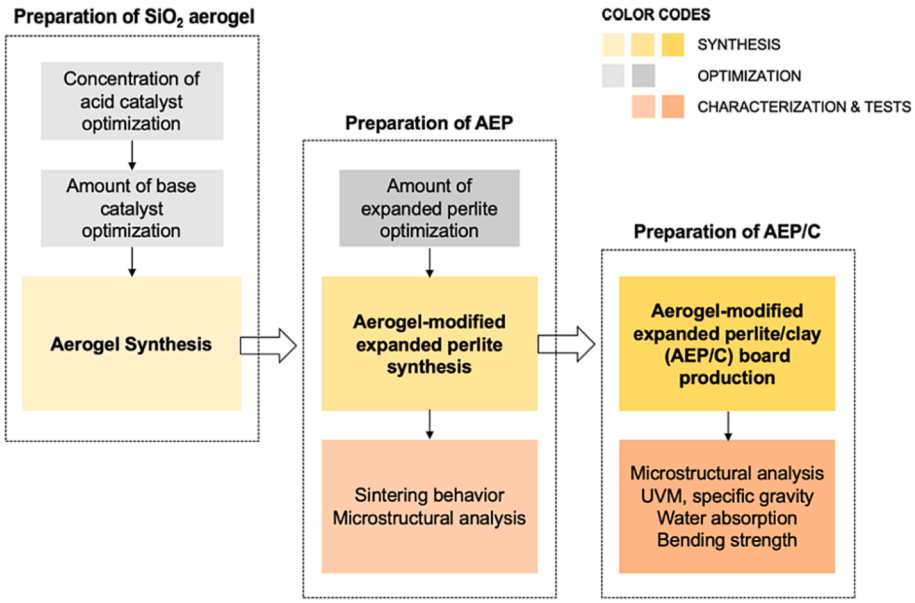

Fig. 1. The flow chart of the design of the study.

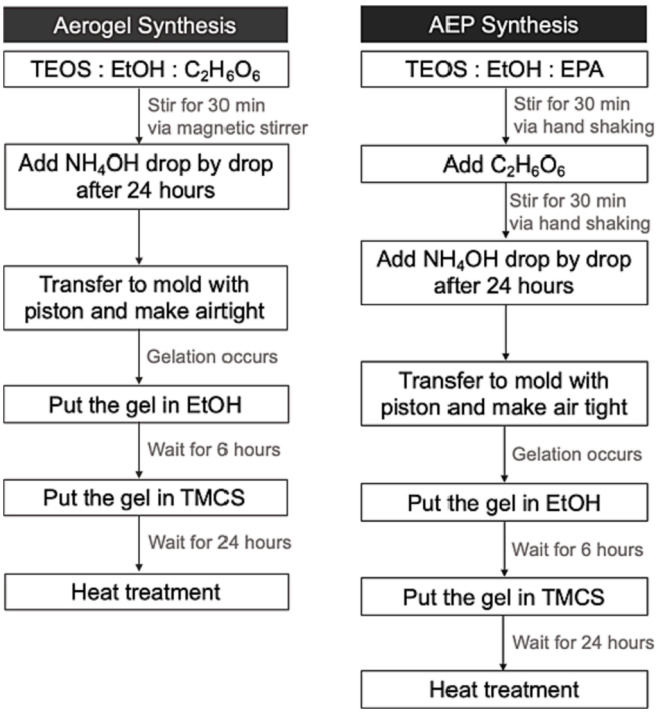

Fig. 2. The schematic of preparation of silica aerogel (left) and AEP (right).

The amount of base catalyst was determined by changing the amount of 1 M ammonia while other chemicals' amounts and molar ratios were fixed. The acid catalyst concentration was kept at 0.02 M, and the molar ratio of TEOS:EtOH:H2O was at 1:5:7. The ammonia amount was varied from 1 ml to 10 ml by 1 ml increment controlled. No gelling was observed, or the gelling duration was very long in the experiments conducted with 1 to 4 ml base catalyst. The 5 ml base catalyst yielded a gelling after a day. The amount of 6 ml and more base catalysts caused rapid gelation, which is undesirable for the time requirement of adequate hydrosol absorption of EPA. The pH measurements were continued during the base catalyst addition. The basic pH values yield nucleation, network formation and growth of aerogels [41,42]. The optimized concentration and amount of acid and base catalysts were used for further studies. The schematic of the aerogel synthesis is illustrated in Fig. 2.

2.3. Preparation of aerogel-modified expanded perlite (AEP)

Determining the amount of EPA and corresponding chemicals required for the modification of perlite is essential for optimizing AEP synthesis. The preparation of AEP was carried out with catalyst concentrations and amounts determined. The 0.02 M acid and 1 M base catalyst with the molar ratio of TEOS:EtOH:H2O were kept constant at 1:5:7. The required amount of EPA was investigated by varying from 10 gr to 45 gr and altered by 5 gr systematically. The sequence was followed in each experiment: EPA was added to the beaker and stirred by hand. The acid catalyst was added to the solution, and the beaker was made airtight. The stirring process was continued for 30 min, and the solution was kept on a vibration-free surface for 24 h. The base catalyst was added dropwise into the stirred beaker. The solution was transferred to the molds with a piston, and they were sealed, as shown in Fig. 3. The samples were removed from the molds after the aging step was completed (Fig. 3 (b)). The samples were washed with EtOH and waited in EtOH solution for 6 h for solvent exchange, then in *n*-hexane:TMCS (5:1 V/V) for 24 h for surface modification. Gels were exposed to 60 °C for 4 h, 80 °C for 2 h, 120 °C for 2 h, and 200 °C for an hour of heat treatment for drying. The optimum amount of EPA for AEP synthesis was determined as 40 g. The schematic of AEP synthesis is shown in Fig. 2 (right).

The high temperatures lead to volume shrinkage and sintering of EPA [43]. The shrinkage causes irremediable deformation of particles. Conversely, SiO_2 aerogels preserve their forms at high temperatures. Therefore, it is expected that the aerogel network inside the perlite and covers the surface protects the structure in high temperatures. Both EPA and AEP particles were exposed to 1100 °C for 4 h. The size of the EPA and AEP particles before heat treatment was < 3 mm. Both particles were sieved from different sieve sizes after the heat treatment. EPA particles yielded considerable volume shrinkage, could pass through a < 2 mm sieve, and their color changed to pink depending on the sintering after the heat treatment. On the other hand, The AEP particles conserved their yellowish/white colors, particles could only pass through a < 3 mm sieve and no volume or form changes were observed.

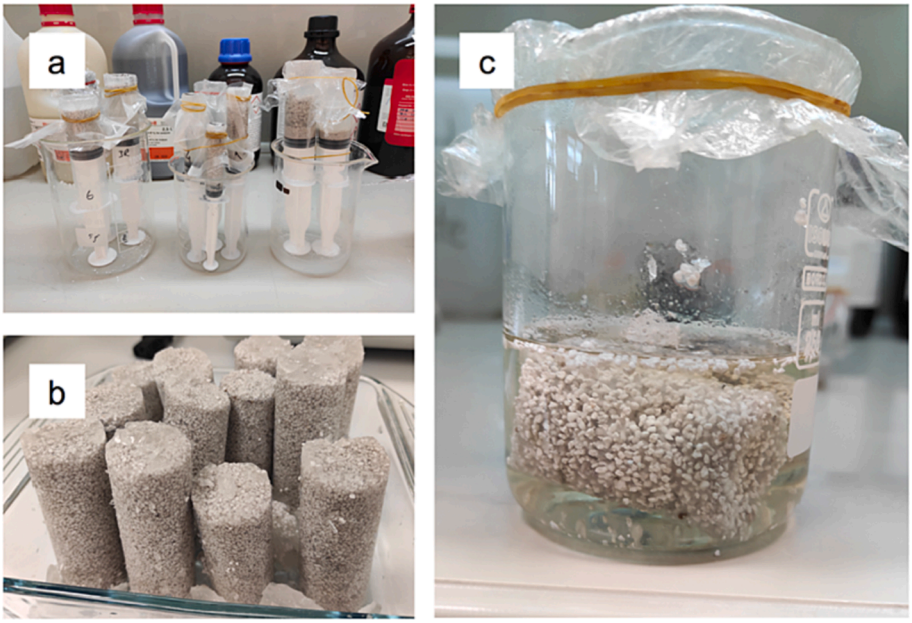

Fig. 3. (a) Photographs of samples in sealed molds, (b) samples ejected from the molds, and (c) the sample in EtOH.

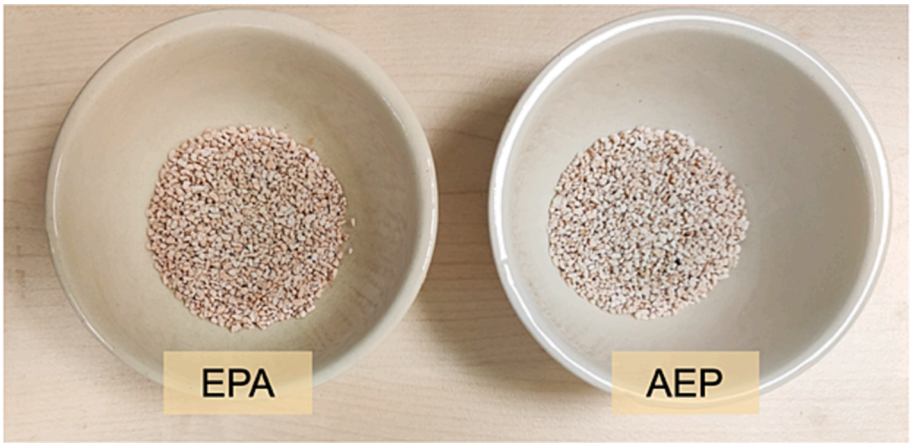

Fig. 4. The photo of EPA and AEP particles after the heat treatment. The color of EPA particles changed from yellow/white to pinkish color. (For interpretation of the references to color in this figure legend, the reader is referred to the web version of this article.)

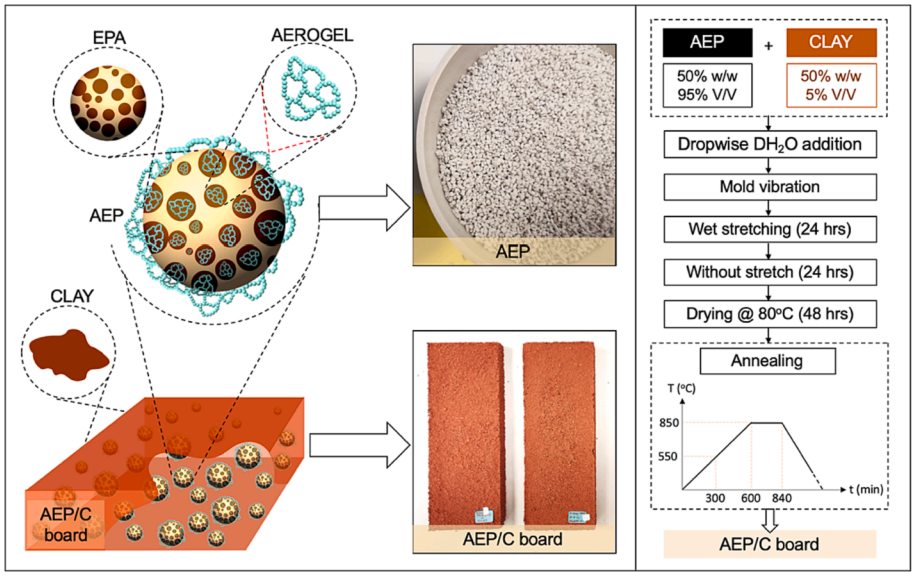

Fig. 5. The representation and photos of AEP and AEP/C composite board. The preparation of aerogel-modified expanded perlite/clay composite board schematic prepared in the light of the study of Yılmazer and Baytekin [37].

The photos of EPA and AEP particles are shown in Fig. 4.

2.4. Preparation of aerogel-modified expanded perlite/clay (AEP/C) board

In the production of AEP/C composite boards, aerogel was employed as a filler, and clay was used as a binder material (Fig. 5). Clay was ground into powders and through a < 0.5 mm mesh sieve. Both perlite and clay have a high potential to catch the humidity of the environment; hence they were exposed to drying at 105 °C until no weight changes were observed. A previous study represents the optimum composition and corresponding process of EP/clay-based exterior wall thermal insulation board. The ratios are 1:1 (W/W) and 1:19 (V/V) for clay and EPA, respectively [44]. In parallel with this study, equal weights of EPA and clay were used to produce EPA/C board as a control sample. Similarly, equal amounts of clay and AEP were weighted with precision balance and were filled into a soft container. It was shaken by hand until obtaining the homogeneous dry mixture. The mixture was transferred to the vessel and water was added drop by drop while stirring until the viscosity of clay and AEP was sustained. The desired viscosity was obtained with 2:3 (V/V) for EPA:DH_2O. The slurry was transferred to the wooden mold and placed on the vibration machine to settle particles for 5 min. The mold was covered with a film layer to make it airtight and keep the natural humidity for 24 h, then followed uncovered waiting for 24 h for the slow vaporization of the water molecules. It was exposed for 48 h drying at 80 °C. The board was ejected from the mold, and the annealing was carried. This annealing process comprises 5 h of gradually increased heating up to 550 °C, then 5 h from 550 to 850 °C. The constant heating at 850 °C was carried out for 4 h, and the cooling was allowed until reaching room temperature. The preparation of the AEP/C board is summarized in illustration in Fig. 5.

2.5. Unit volume mass and specific gravity of AEP/C board

Unit volume mass is calculated by dividing the weight by the volume containing the voids. The boards were weighted and dimensions were determined with 0.1 mm precision. The dimensions of the produced boards were 19.9 ± 0.1 cm * 7.7 ± 0.2 cm * 1.8 ± 0.1 cm. UVM of boards was calculated according to the following equation.

$$UVM = m/V \text{ and } V = l^{*}b^{*}d$$

On the other hand, specific gravity (SG) is calculated by dividing the

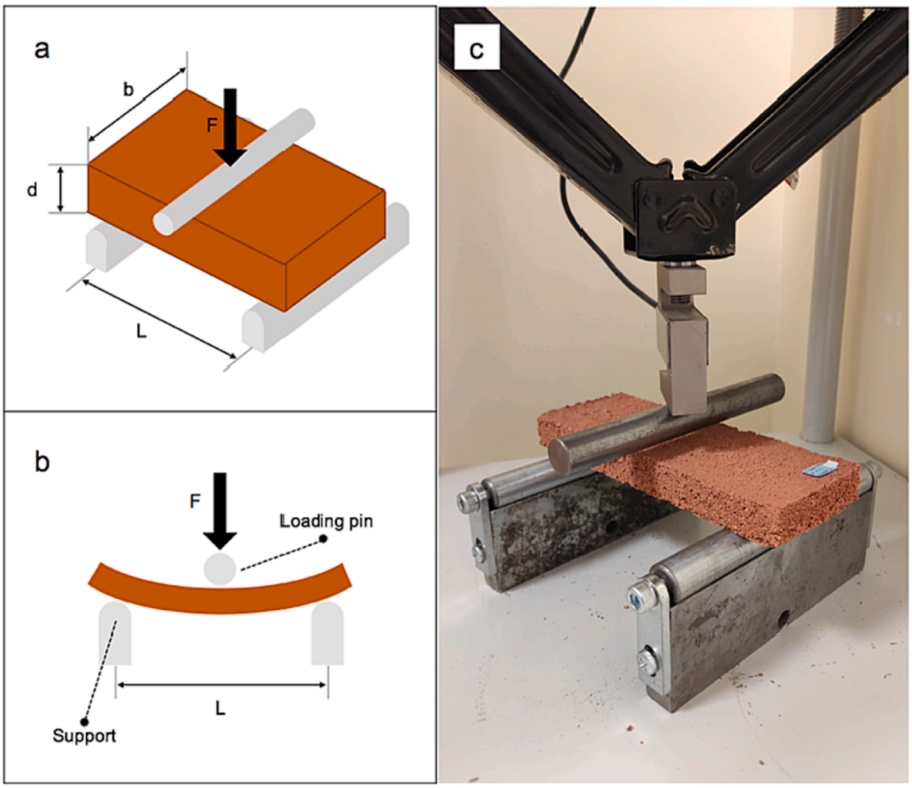

Fig. 6. (a) The axonometric representation and (b) side view of a schematic of flexural strength, and (c) the photograph of the bending test machine and the board before testing.

weight by the volume without the voids. For this reason, the boards were ground into powders and were dried at 110 ± 5 °C in the oven until constant weight. They carefully poured into the Le Chatelier flask under the light of TS 2511 standard [45]. The equation for SG is following:

$$SG = W/V_C$$

2.6. Morphological analysis of AEP/C

The internal microstructure of AEP/C boards was observed using FEI scanning electron microscopy (SEM). For the preparation, the boards were cut carefully, and cross-section samples were placed on the SEM pins. They were coated with the gold/ palladium (Au/Pd) in the sputtering device to prevent the charging of samples under electron bombardment and high vacuum inside SEM. They were examined under 5 kV.

2.7. Water absorption

Considering that the thermal conductivity of water is at an undesirable level, inorganic materials will show even higher thermal conductivity in a humid environment [27]. Expanded perlite aggregate has a uniformly distributed microvesicular texture that allows water molecules to vaporize quickly from pores while a small degree of expansion occurs [22]. On the other hand, the inclusion of water into the pores of EPA causes an increase in heat conductivity, therefore undesirable thermal insulation properties [38]. Thus, the water absorption capacity test is significant for the material to analyze the suitability of the construction, and this capacity gives information about the boards' open porosity.

Water absorption is the percentage of the ratio of absorbed water and the dry weight of the board. The WA tests were conducted according to TS EN ISO 29,767 standard [46]. To measure the dry weight (W_D) of the boards, they were dried at 110 ± 5 °C in the oven until observing the constant weight. The boards were submerged in water for 48 h. They were taken out from the water and weighted (W_W). The following formula calculated the water absorption rates of boards.

$$WA = ((W_W - W_D)/W_D)^* \%$$

The volume of voids is significant in analyzing the volume occupied by the pores after aerogel modification in the boards. The void volume is calculated according to the formula below. $\mathbf{V_V = (SP - \rho / SP) * V}$ where the density was calculated by $\mathbf{\rho = W_D / V_T}$

Porosity was calculated to the equation below.

$$Porosity = (V_V/ V_T)^*100\%$$

2.8. Bending strength/three-point flexural test (bending strength test)

The tensile property shows how much a material reacts to the force before it breaks. The bending strength is the ability to resist deformation under load. The bending behavior was analyzed according to the TS EN 12,089 standard [47]. The strength of boards was determined by bending-stress measuring equipment based on the three-point flexural test, as shown in Fig. 6 (c). The loading force was applied to the middle of the board placed on two parallel supporting points (Fig. 6 (a), (c)). The concave side of the board is exposed to tension, and the convex side is subjected to maximum stress when the force is applied. The board starts to bend concave downwards and fails at the maximum load when the strain or elongation exceeds the material's limits, as illustrated in Fig. 6 (b). The recorded maximum applied force (F) was used in the flexural strength formula of the board [47].

$$\sigma = 3LF/(2bd^2)$$

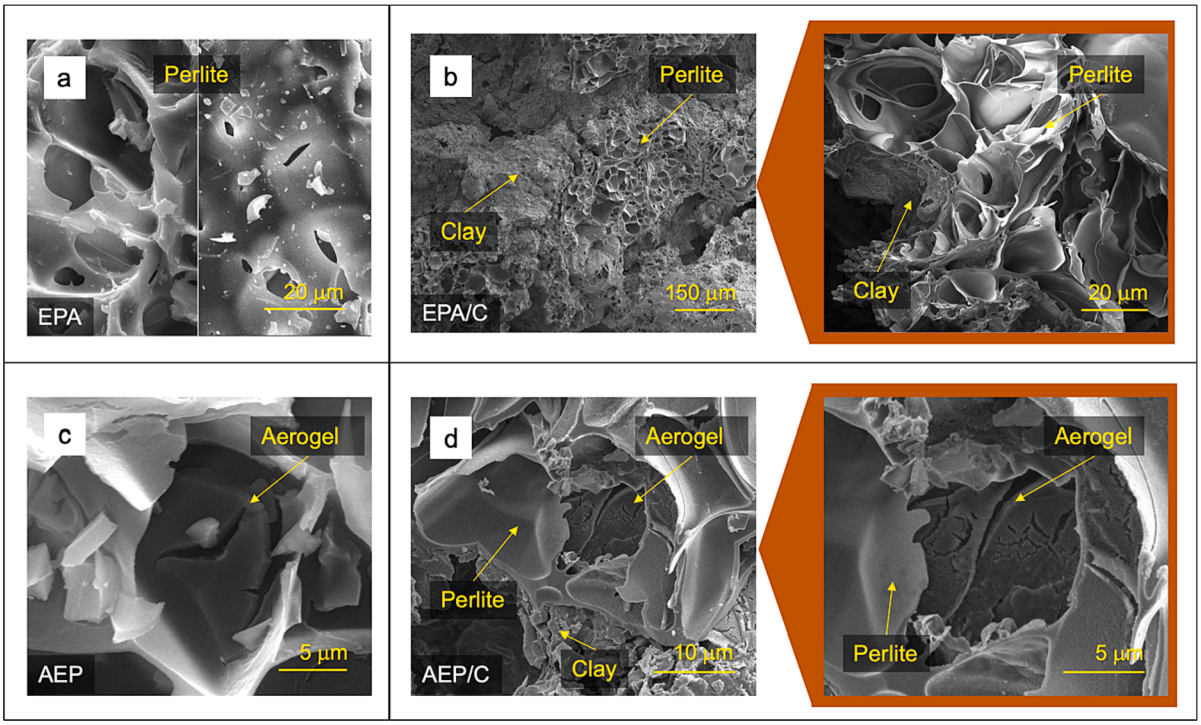

Fig. 7. SEM images of internal surfaces of (a) EPA, (b) EPA/C (control sample board), (c) AEP and (b) AEP/C composite boards. Close-up SEM images are shown on the right side of the images of EPA/C and AEP/C boards.

3. Results and discussion

3.1. Morphology of AEP/C

The SEM images show the internal surface of the EPA/C and AEP/C boards. Many closed cells were opened while cutting the boards for SEM preparation. Therefore, the network of the perlite and clay coverings are observable. As can be seen in Fig. 7 (a), the EPA/C control sample board surface has a three-dimensional cellular network of perlite and rough clay coverings. The EP comprises several pore forms such as spherical pores, slit pores, and irregular wide-opened pores [27]. Clay coverings are observed as an irregular distribution on the surface. Especially, clay penetrates and fills relatively bigger pores, and the small and thin-walled holes preserve their hollow structure. The surface of AEP/C demonstrates open and closed perlite cavities, aerogel inside the perlite holes, and clay coverings around perlite particles, as shown in Fig. 7 (b). SEM images represent that aerogel fills into the perlite pores and covers the surfaces of the aggregates. This image was very similar to the study of Jia et al. [27]. The surface of the aerogel in our study resembled the study of Peng & Yang [35]. In this study, the rough aerogel structure inside the aerogel/EP composite was given in the SEM images. Clay is the binder, and aerogel is a filler material in our study. The clay matrix covers the outer shell surfaces of the AEP particles and keeps them together throughout the board. In contrast with the control sample board of EPA/C, open perlite cavities are filled with aerogel in AEP/C boards. The active hydrolysis and condensation reactions occurred between the cavities, and the three-dimensional web structure was obtained for the aerogel formation [28,41]. This means that aerogel is developed inside the perlite holes and covers the surfaces of the perlite particles. Therefore, aerogel modification blocks the clay penetration into the perlite pores. As seen in Fig. 7, clay coverings are observed only on the shell surfaces of AEP and between AEP particles.

3.2. Unit volume mass and specific gravity AEP/C board

The volume in the UVM calculation comprises both the solid and void volume of the boards. Clay occupies the gaps between the particles packed according to the Kepler conjecture. Nevertheless, clay is used as a binder in both the EPA/C control board and AEP/C board composite. Therefore, the gap volume between packed particles is filled with clay in both composites. According to Fig. 7, in AEP/C composite, aerogel coats the shell surfaces of perlite particles and fills some of the open pores of the perlites. This means aerogel also substitutes some of the relatively smaller pores of particles that clay does not occupy. Therefore, aerogel modification slightly increases the weight and UVM of the AEP/C board compared to the EPA/C composite. The UVM of the control board of EPA/C was calculated as 0.46 ± 0.02 g/cm^3. On the other hand, AEP/C board UVM was found as 0.55 ± 0.01 g/cm^3. The change can be explained by the synthesized aerogel having a more dense crosslinking than the EPA's porous structure.

The SG considers the solid volume without voids. The SG of the EPA/C control board was calculated as 2.33 ± 0.02 g/cm^3 and AEP/C was 2.36 ± 0.01 g/cm3. Aerogel modification of particles slightly affected the specific gravity of the boards as compared to aerogel-free control boards. This slight difference between boards can be ignored. On the other hand, UVM and SG of the EPA/C control board were higher than the expanded perlite/clay-based board in the previous study by Yılmazer [44]. The same clay was used in both studies; however, the source region and perlite particle size determine composite boards' properties.

The slight difference between UVMs of EPA/C and AEP/C in our study leads to point out the advantages in two aspects: The first advantage is that it is likely that the aerogel modification of perlite does not yield a remarkable additional weight on AEP/C composites. Secondly, sustaining the low UVM values significant in determining the thermal properties of porous materials, even the sound absorption coefficient [44,48]. The aerogel modification leads to an indistinct change in the UVM value and indicates that it would not cause a noticeable effect on the thermal resistivity via density-related variables [37]. On the other hand, the thermal conductivity of aerogel is often lower than air, and the aerogel modification causes the replacement of the SiO_2 network with the air in the pores [28,42]. Therefore, it can be presumed that the AEP/C composite may have approximately equal or lower

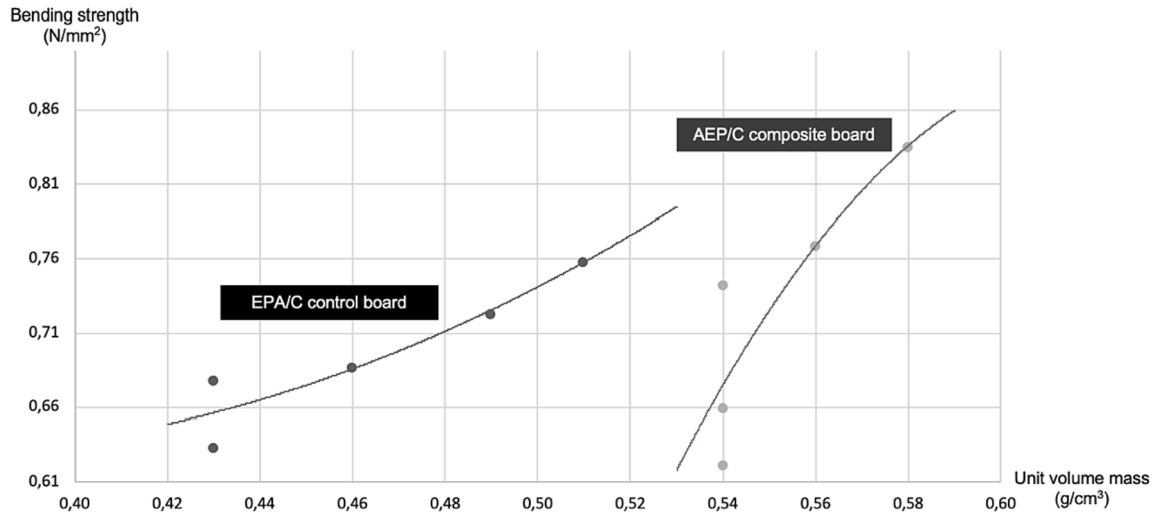

Fig. 8. The specific gravity and bending strength of EPA/C and AEP/C composite boards.

thermal conductivity than the EP/C control board. Thus, the thermal conductivity measurement of the produced boards is needed to confirm this inference.

3.3. Water absorption

The *volume of voids* is 40.5 and 36.23 ± 1.05 for the EPA/C control board and the AEP/C board, respectively. Aerogel has a highly porous solid 3D network that supports mechanical strength, low thermal conductivity, and high moisture retention ability [42]. Therefore, aerogel tenuously fills open pores of perlite, although it penetrates most of the open pores and covers the surfaces of perlite. Therefore, the volume of voids seems to decrease with the aerogel modification slightly. On the other hand, the *porosity* shows the percentage of the total void volume of the boards. Calculations reveal that the porosity of the control board was 0.78 % and 0.77 % for AEP/C. The results were accepted as the porosities of the AEP/C and control boards are equal. The volume of voids and porosity calculations approved the aerogel's intrinsic porous structure. The continuity of the total porosity was provided after the aerogel modification. On the other hand, the previous study stated that the porosity of the EPA/C board was 0.87 % [39]. This is related to the perlite source dependency of the porosity.

It has been long known that moisture catching is a disadvantage in plates made of porous materials, and studies have been carried out on water retarding properties of plates made of perlite [48]. Therefore, using moisture-repellent, hydrophobic porous material plates in buildings is an advantage [49,50]. However, it should be emphasized that it is advantageous for the end-product to be hydrophobic. The hydrophobic aerogel production methods are widely studied in the literature [32,50]. On the other hand, the hydrophobic materials are unsuitable for wet synthesis methods such as our composite production process [51]. The clay and the aerogel-modified perlite are mixed as a slurry and are molded. If the aerogel is hydrophobic, the clay would not completely wrap and bind to the aerogel-modified perlite. The hydrophobic surface of aerogel causes agglomeration of AEP particles in the slurry to repel from the water. This would cause compatibility deterioration between clay and the AEP particles, reducing the board composite's mechanical strength. Therefore, the aerogel's acceptable hydrophilic behavior and water absorption capacity are favorable for our board production. The water absorption calculations reveal that the EPA/C control board was 86.28 %. Since the aerogel modification, the absorption capacity of the AEP/C board was slightly decreased to 83.91 ± 0.49 %. Hence observing that water absorbance did not increase in the aerogel-modified plates is promising for future research.

3.4. Bending strength

The mean flexural strengths of five EPA/C control boards was 0.70 ± 0.02 N/mm^2, and five of AEP/C was 0.73 ± 0.04 N/mm^2. As mentioned above, the mean UVM of control samples was 0.46 ± 0.02 g/cm^3, and AEP/C boards was 0.55 ± 0.01 g/cm^3. The correlation between the UVM and bending strength of the composite boards are shown in Fig. 8. Upon closer inspection, the ascending UVM values for both EPA/C and AEP/C boards tend to increase on the flexural strength with a general trend parallel with the previous study [37]. The common point with our study is that the bending strength rose as the UVM increased in the EPA/C composite [39,44]. In this study, the bending strength of the EPA/C board was 0.52 N/mm^2; however, our study asserts that the EPA/C board with 0.70 ± 0.02 N/mm^2. The difference depends on the particle size and the source of perlite, thus the binding performance. The second reason can be the cooling duration difference in the annealing processes. The annealing process up to the cooling step is the same as in the previous study. However, the cooling period from 850 °C to room temperature without any intervention is significant in determining the boards' mechanical performance. The long cooldown periods lead the boards to be cured by being exposed to these temperatures for a long time. In our study, there was no disturbance until the boards reached room temperature. Hence the furnace we used has determined the period of the cooling process. Therefore, the extended cooling period may lead the boards to be exposed to a longer curing period than in the previous study. Thus, we observed that the boards had higher UVM values due to staying in the cooling phase for longer.

If we were to compare EPA/C and AEP/C boards, the tentative increase in UVM means (~0.09 g/cm^3) caused ~ 0.03 N/mm^2 increase in the flexural strengths. In other words, the mild change on the UVM depended on the aerogel modification; however, the bending strength of the boards was almost equal to each other. On the other hand, even two of the control boards have the same UVM value (0.43 g/cm^3), they exhibited very close but slightly different strength values as 0.63 N/mm^2 and 0.68 N/mm^2. Similarly, an upward trend was observed for AEP/C composites. Three boards have UVM with 0.54 g/cm^3 had a different bending strength of 0.62, 0.66, and 0.74 N/mm^2. The slight UVM increase, 0.56 g/cm^3 corresponds to bending strength 0.77 N/mm^2, 0.58 g/cm^3 had 0.84 N/mm^2. While UVM and bending strength showed an upward trend together, the fact that three boards with the same UVM value had different bending strengths is related to the experimental conditions during the board preparations. For example, mixing the slurry and pressing the mortar in the mold after the vibration step for the particle settlement can cause surface defects and differences in

Table 2
The ratios for board preparation, physical and mechanical test results of EPA/C and AEP/C boards.

Physical and mechanical test results								
Property	Perlite: Clay	Unit volume mass (UVM)	Density (ρ)	Specific gravity (SP)	Volume of voids (V_V)	Porosity (n)	Water absorption (WA)	Bending strength (σ)
Unit / Sample	W/W		g/cm^3	g/cm^3	cm^3	%	%	N/mm^2
EPA/C (Control sample)	1:1	0.46 ± 0.01	0.51	2.33 ± 0.02	40.51	0.78	86.28	0.70 ± 0.02
AEP/C	1:1	0.55 ± 0.01	0.55	2.36 ± 0.01	36.23 ± 0.01	0.77	83.91 ± 0.49	0.73 ± 0.04

structural homogeneities between the boards. Cracks inside and on the surfaces can cause the boards to break with less force than expected. As it is known, extra squeezing pressure applied to the mortar in the mold yields a rise in both UVM and the strength of the boards. However, it was concluded that the flexural strength value that the UVM of the board should provide is lower than anticipated. It should be taken into account that the UVM discrepancies between the boards were minimal and caused mild differences in the bending strengths. Although the possibility of human-related errors, the general trend of the boards is ascending bending strength with increasing UVM values. In addition, researches demonstrate that aerogel addition to the mixture leads to a decrease in mechanical strength [52]. Although our results seem consistent with studies involving composites prepared with aerogel reinforcement, the differences in flexural strength in previous studies are very obvious. In our study, the difference in flexural strength of the aerogel-modified board and unmodified board is negligible. This is one of the prominent results of this study. The mixing ratios in weight for the preparation of the boards and corresponding physical and mechanical characterization results of the EPA/C and AEP/C composited are shown in Table 2.

4. Conclusion

The clay-based aerogel-modified expanded perlite composite board was prepared and physical and mechanical properties investigated in this study. In order to synthesize aerogel at ambient pressure, a two-step acid-base catalyzed sol–gel method was used. Silica aerogels were prepared with systematic variation in the amount of acid catalyst and the concentration of the base catalyst. The modification was considered filling the open pores and coating expanded perlite with the synthesized silica aerogel. Therefore, the optimum amount of perlite was determined by altering systematically. The results indicated that the optimum conditions for the aerogel modification of expanded perlite were 10 ml 0.02 M acid catalyst, 5 ml 1 M base catalyst with 40 gr EPA by keeping the molar ratio of TEOS:EtOH:H_2O constant at 1:5:7. The prepared particles allowed a homogeneous mixing of the clay and water slurry for board production. The physical and mechanical tests were conducted according to TS 2511, TS EN ISO 29,767 and TS EN 12,089 standards. Considering the physical and mechanical properties, the resulting aerogel-modified expanded perlite and clay (AEP/C) boards possessed slight differences from boards prepared without modification of expanded perlite. Calculations revealed that the modification faintly reduced the void volume of the boards to 36.23 ± 1.05, and water absorption capacity to 83.91 ± 0.49 % consequently. The porous structure of the perlite was preserved while specific gravity and unit volume mass slightly increased to 2.36 ± 0.01 and 0.55 ± 0.01 g/cm^3, respectively. This resulted in a negligible change to 0.73 ± 0.04 N/mm^2 in the flexural strengths of the composite boards. The bending strength results also validated the AEP/C board preparation at high temperatures without perlite sintering.

This study is the pioneer in investigating aerogel/EPA board properties with a clay matrix. The future direction of this study can be examining the thermal performance of the boards. Previous studies presented the potentiality of clay-based EPA boards' usage as thermal insulation boards [37,39]. Considering the low thermal conductivity of the aerogel; this work can be a candidate a thermal insulation material in buildings for energy saving in the future. As it is known, EPA and aerogel are well-known lightweight insulation materials, however, it is hard to produce them in board form because of the handling difficulties [25,28]. The limitation of this work is low mechanical strength than the limit strength value for using a board in construction. Using this new route suggested in this work, an insulation board can be produced by including lightweight materials and composite with low thermal conductivity in the perlite, aerogel, and clay mixture to improve mechanical strength with desired performances.

Funding

No funding was received for conducting this study.

7. Availability of data and material

All authors ensure that all data and materials support their published claims and comply with field standards.

8. Code availability

Not applicable

9. Authors' contributions

All authors contributed to the study's conception and design. The first draft of the manuscript was written by Elif Mercan, and all authors commented on previous versions of the manuscript. All authors read and approved the final manuscript.

Declaration of Competing Interest

The authors declare that they have no known competing financial interests or personal relationships that could have appeared to influence

the work reported in this paper.

Data availability

Data will be made available on request.

Acknowledgments

The authors are thankful UNAM-National Nanotechnology Research Center for laboratory opportunities.

References

[1] K. Kalhor, N. Emaminejad, Qualitative and quantitative optimization of thermal insulation materials: Insights from the market and energy codes, J. Build. Eng. 30 (2020), 101275, https://doi.org/10.1016/j.jobe.2020.101275.
[2] I.Z. Bribián, A.V. Capilla, A.A. Usón, Life cycle assessment of building materials: Comparative analysis of energy and environmental impacts and evaluation of the eco-efficiency improvement potential, Build. Environ. 46 (5) (2011) 1133–1140, https://doi.org/10.1016/j.buildenv.2010.12.002.
[3] L. Aditya, T.M.I. Mahlia, B. Rismanchi, H.M. Ng, M.H. Hasan, H.S. Metselaar, O. Muraza, H.B. Aditiya, A review on insulation materials for energy conservation in buildings, Renew. Sustain. Energy Rev. 73 (2017) 352–1365, https://doi.org/10.1016/j.rser.2017.02.034.
[4] H.Y. He, Y. Chu, Y. Song, M. Liu, S. Shi, X. Chen, Analysis of design strategy of energy efficient buildings based on databases by using data mining and statistical metrics approach, Energy Build. 258 (4) (2021), 111811, https://doi.org/10.1016/j.enbuild.2021.111811.
[5] G. Ioppolo, S. Cucurachi, R. Salomone, G. Saija, L. Shi, Sustainable local development and environmental governance: a strategic planning experience, Sustain. 8 (2) (2016) 180, https://doi.org/10.3390/su8020180.
[6] O. Ortiz, F. Castells, G. Sonnemann, Sustainability in the construction industry: a review of recent developments based on LCA, Constr. Build. Mater. 23 (1) (2009) 28–39, https://doi.org/10.1016/j.conbuildmat.2007.11.012.
[7] J. Coma, G. Pérez, C. Solé, A. Castell, L.F. Cabeza, Thermal assessment of extensive green roofs as passive tool for energy savings in buildings, Renew. Energy 85 (2016) 1106–1115, https://doi.org/10.1016/j.renene.2015.07.074.
[8] F. Chen, Y. Zhang, J. Liu, X. Wang, P.K. Chu, B. Chu, N. Zhang, Fly ash based lightweight wall materials incorporating expanded perlite/SiO_2 aerogel composite: Towards low thermal conductivity, Constr. Build. Mater. 249 (2020), https://doi.org/10.1016/j.conbuildmat.2020.118728.
[9] M. Ibrahim, K. Nocentini, M. Stipetic, S. Dantz, F. Caiazzo, H. Sayegh, L. Bianco, Multi-field and multi-scale characterization of novel super insulating panels/systems based on silica aerogels: Thermal, hydric, mechanical, acoustic, and fire performance, Build. Environ. 151 (2019) 1–3, https://doi.org/10.1016/j.buildenv.2019.01.019.
[10] A. Papadopoulos, E. Giama, Environmental performance evaluation of thermal insulation materials and its impact on the building, Build. Environ. 42 (55) (2007) 2178–2187, https://doi.org/10.1016/j.buildenv.2006.04.012.
[11] M. Taherishargh, I.V. Belova, G.E. Murch, T. Fiedler, Low-density expanded perlite-aluminium syntactic foam, Mater. Sci. Eng. A 604 (2014) 127–134, https://doi.org/10.1016/j.msea.2014.03.003.
[12] Y. Lin, X. Li, Q. Huang, Preparation and characterization of expanded perlite/wood-magnesium composites as building insulation materials, Energy Build. 231 (6) (2021), 110637, https://doi.org/10.1016/j.enbuild.2020.110637.
[13] A.M. Rashad, A synopsis about perlite as building material - A best practice guide for Civil Engineer, Constr. Build. Mater. 121 (2016) 338–353, https://doi.org/10.1016/j.conbuildmat.2016.06.001.
[14] O. Gencel, O. Bayraktar, G. Kaplan, M. Nodehi, A. Benli, A. Gholampour, T. Ozbakkaloglu, O. Arslan, Lightweight foam concrete containing expanded perlite and glass sand: Physico-mechanical, durability, and insulation properties, Constr. Build. Mater. 320 (2022), 126187, https://doi.org/10.1016/j.conbuildmat.2021.126187.
[15] R. Demirboga, R. Gul, The effects of expanded perlite aggregate, silica fume and fly ash on the thermal conductivity of lightweight concrete, Cem. Concr. Res. 33 (5) (2003) 723–727, https://doi.org/10.1016/S0008-8846(02)01032-3.
[16] A. Karaipekli, A. Sari, K. Kaygusuz, Thermal characteristics of paraffin/expanded perlite composite for latent heat thermal energy storage, Energy Sour. Part A 10 (2009) 814–823, https://doi.org/10.1080/15567030701752768.
[17] N. Zhang, Y. Yuan, Y. Yaguang, L. Tianyu, L., X. Cao., Lauric–palmitic–stearic acid/expanded perlite composite as form-stable phase change material: Preparation and thermal properties, Energy Build. 82 (2014) 505–511, https://doi.org/10.1016/j.enbuild.2014.07.049.
[18] H. Binici, F. Kalaycı, Production of perlite based thermal insulation material, Int. J. Acad. Res. Reflect. 3 (7) (2015) 47–54.
[19] E.T. Dawood, Experimental study of lightweight concrete used for the production of canoe, Al-Rafidain Eng. J. 23 (2) (2015) 96–106. https://doi.org/10.33899/rengj.2015.101085.
[20] M. Lanzón, P.A. García-Ruiz, Lightweight cement mortars: Advantages and inconveniences of expanded perlite and its influence on fresh and hardened state and durability, Constr. Build. Mater. 22 (8) (2008) 1798–1806, https://doi.org/10.1016/j.conbuildmat.2007.05.006.
[21] Y. Maaloufa, S. Mounir, A. Khabbazi, J. Kettar, A. Khaldoun, Thermal characterization of materials based on clay and granular: cork or expanded perlite, Energy Procedia 74 (2015) 1150–1161, https://doi.org/10.1016/j.egypro.2015.07.757.
[22] H. A. Haery. Elastic and mechanical properties of expanded perlite and perlite/epoxy foams (Doctoral dissertation) (2017). https://ogma.newcastle.edu.au/vital/access/manager/Repository/uon:28964.
[23] B. Işıkdağ, B. Topçu, S. Gökbel, Characterization of mortars produced with expanded perlite, slaked lime and waste tile dust, Iwcea Özel Sayisi 1 (2015) 29–42.
[24] S.A. Yıldızel, Mechanical performance of glass fiber reinforced composites made with gypsum, expanded perlite and silica sand, Romanian J. Mater. 48 (2018) 229–235.
[25] M. Koebel, A. Rigacci, P. Achard, Aerogel-based thermal superinsulation: An overview, J. Sol-Gel Sci. Technol. 63 (3) (2012) 315–339, https://doi.org/10.1007/s10971-012-2792-9.
[26] N. Sakiyama, J. Frick, M. Stipetic, T. Oertel, H. Garrecht. Hygrothermal performance of a new aerogel-based insulating render through weathering: Impact on building energy efficiency. Build. Envir. 202 (5-6) (2021) 108004. 108004. 10.1016/j.buildenv.2021.108004.
[27] G. Jia, Z. Li, P. Liu, Q. Jing, Preparation and characterization of aerogel/expanded perlite composite as building thermal insulation material, J. Non-Cryst. Solids 482 (2018) 192–202, https://doi.org/10.1016/j.jnoncrysol.2017.12.047.
[28] Q. Yan, Z. Feng, J. Luo, W. Xia, Preparation and characterization of building insulation material based on SiO2 aerogel and its composite with expanded perlite, Energy Build. 255 (2021), 111661, https://doi.org/10.1016/j.enbuild.2021.111661.
[29] R. Baetens, B. Jelle, A. Gustavsen, Aerogel insulation for building applications: A state-of-the-art review, Energy Build. 43 (4) (2011) 761–769, https://doi.org/10.1016/j.enbuild.2010.12.012.
[30] T. Burger, J. Fricke, Aerogels: Production, modification and applications, Berichte der Bunsengesellschaft/Phys. Chem. Chem. Phys. 102 (11) (1998) 1523–1528, https://doi.org/10.1002/bbpc.19981021102.
[31] M. Stefanidou, V. Pachta. Influence of perlite and aerogel addition on the performance of cement-based mortars at elevated temperatures. IOP Conference Series: Earth Envir.Sci. 410 (1) (2020) 10.1088/1755-1315/410/1/012111.
[32] S. Shang, X. Ye, X. Jiang, Q. You, Y. Zhong, X. Wu, S. Cui, Preparation and characterization of cellulose/attapulgite composite aerogels with high strength and hydrophobicity, J. Non-Cryst. Solids 569 (2021), 120922, https://doi.org/10.1016/j.jnoncrysol.2021.120922.
[33] L. Wang, P. Liu, Q. Jing, Y. Liu, W. Wang, Y. Zhang, Z. Li, Strength properties and thermal conductivity of concrete with the addition of expanded perlite filled with aerogel, Constr. Build. Mater. 188 (2018) 747–757, https://doi.org/10.1016/j.conbuildmat.2018.08.054.
[34] V.A. Rao, S.D. Bhagat, Synthesis and physical properties of TEOS-based silica aerogels prepared by two-step (acid-base) sol-gel process, Solid State Sci. 6 (9) (2004) 945–952, https://doi.org/10.1016/j.solidstatesciences.2004.04.010.
[35] K. Peng, H. Yang, Preparation of aerogel-modified expanded perlite and its application in heat insulation coating, Adv. Mater. Res. 668 (2013) 360–364, https://doi.org/10.4028/www.scientific.net/AMR.668.360.
[36] G. Jia, Z. Li, Influence of the aerogel/expanded perlite composite as thermal insulation aggregate on the cement-based materials: Preparation, property, and microstructure, Constr. Build. Mater. 273 (2021), 121728, https://doi.org/10.1016/j.conbuildmat.2020.121728.
[37] S. Yılmazer, B. Baytekin. The mixture ratio optimization of expanded perlite-clay based board (EPcB) for thermal resistance performance. International Porous Powder Materials Symposium and Exhibition (PPM), İzmir Institute of Technology (2017) September,12-15. Kuşadası, İzmir, Turkey.
[38] I.B. Topçu, B. Işikdağ, Manufacture of high heat conductivity resistant clay bricks containing perlite, Build. Environ. 42 (10) (2007) 3540–3546, https://doi.org/10.1016/j.buildenv.2006.10.016.
[39] S. Yilmazer. The chemical synthesis and process optimization of a porous thermal insulation board made of clay based expanded perlite (EPcB). International Porous Powder Materials Symposium and Exhibition (PPM) (2019) October, 9-11. Marmaris, Muğla, Turkey.
[40] Z.B. Öztürk, Effect of addition of Avanos's (Nevşehir) clays on physical and microstructure of ceramic tile, J. Australian Ceram. Soc. 53 (2017) 101–107.
[41] C.J. Brinker, G.W. Scherer, Sol-gel science, the physics and chemistry of sol-gel processing, CA, Academic Press, San Diego, 1990.
[42] S.A. Dorcheh, M.H. Abbasi, Silica aerogel; synthesis, properties and characterization, J. Mater. Process. Technol. 199 (1) (2008) 10–26, https://doi.org/10.1016/j.jmatprotec.2007.10.060.
[43] B. Skubic, M. Lakner, I. Plazl, Sintering behavior of expanded perlite thermal insulation board: modeling and experiments, Ind. Eng. Chem. Res. 52 (30) (2013) 10244–10249, https://doi.org/10.1021/ie400196z.
[44] S. Yilmazer. The optimization of thermal insulation board made of clay based expanded perlite (EPcB). TUBITAK 1001 Project Final Report, 2018.
[45] TS 2511. Mix design for structural lightweight aggregate concrete.
[46] TS EN ISO 29767. Thermal insulating products for building applications - Determination of short-term water absorption by partial immersion.
[47] TS EN 12089. Thermal insulating products for building applications-Determination of bending behavior.
[48] S. Yilmazer, M. Özdeniz, The effect of moisture content on sound absorption of expanded perlite plates, Build. Environ. 40 (2005) 311–318, https://doi.org/10.1016/j.buildenv.2004.07.004.

[49] C. Shi, H. Zhang, Y. Xuan, Experimental investigation of thermal properties and moisture buffering performance of composite interior finishing materials under different airflow conditions, Build. Environ. 160 (8) (2019), https://doi.org/10.1016/j.buildenv.2019.106175.
[50] S. Ng, B.P. Jelle, T. Stæhli, Calcined clays as binder for thermal insulating and structural aerogel incorporated mortar, Cem. Concr. Compos. 72 (2016) 213–221, https://doi.org/10.1016/j.cemconcomp.2016.06.007.
[51] S. Ng, B. P. Jelle, L. I. C. Sandberg, T. Gao, Ó.H. Wallevik. Experimental investigations of aerogel-incorporated ultra-high performance concrete. Constr. Build. Mater. 77 (2015) 307–316. 10.1016/ j.conbuildmat.2014.12.064.
[52] S. Shah, K.H. Mo, Y. Soon Poh, M. Radwan, Effect of micro-sized silica aerogel on the properties of lightweight cement composite, Constr. Build. Mater. 290 (9) (2021), 123229, https://doi.org/10.1016/j.conbuildmat.2021.123229.